

Effect of Heat Treatment on the Microstructure and Hardness of Novel Ti-6Al-6Mo Alloy Formed by Laser Solid Forming

Zhang Fengying¹, Hu Tengpeng¹, Tan Hua², Qiu Ying¹, Mei Min¹, Yang Haiou²

¹ Chang'an University, Xi'an 710064, China; ² State Key Laboratory of Solidification Processing, Northwestern Polytechnical University, Xi'an 710072, China

Abstract: A novel Ti-6Al-6Mo alloy sample was fabricated by laser solid forming (LSF) using blended elemental powders as raw material. The microstructure of the as-deposited sample was investigated, and the effects of solution and aging treatment on the microstructure and microhardness of LSF Ti-6Al-6Mo alloy were discussed. The results show that the heat treatment conducted in this study has no obvious effect on the morphologies of prior β grains of the alloy. The solution temperature, solution time, and cooling method after solution treatment have a significant effect on the morphology and size of α phase in the prior β grains and the microhardness of the LSF Ti-6Al-6Mo alloy. When the aging time exceeds 4 h, the microstructure and microhardness of the alloy change little with aging time. Based on the precipitation mechanism of the primary α laths and secondary α laths and their strengthening effect on the β matrix in LSF Ti-6Al-6Mo alloy under different heat treatment conditions, the influence mechanism of heat treatment on the microstructure and microhardness of LSF Ti-6Al-6Mo was revealed.

Key words: laser additive manufacturing; Ti-6Al-6Mo; heat treatment; microstructure; microhardness

Laser solid forming (LSF), also known as direct metal deposition (DMD)^[1], laser melting deposition (LMD)^[2] or laser metal deposition (LMD)^[3,4], is a promising free-form additive manufacturing technology that combines the advantages of rapid prototyping and laser cladding. With its unique capacity of fabricating metallic components without using mold, LSD provides the capability of fabricating geometrically complex components that are difficult to fabricate via traditional processing techniques. These significant advantages make LSF an ideal approach for fabricating complex components with superalloys and refractory metals, which are major structural materials and which can be used to fabricate turbine blades in advanced aircraft engines. The LSF process also allows for the flexibility of depositing a blend of elemental powders and of creating an alloy in the process since the powders can be injected into the melt pool

synchronously. It can also be used to investigate new alloy systems and to create functional structures and innovative materials^[5,6].

Titanium and titanium alloys are extensively used in aviation, aerospace, marine, and biomedical applications due to their excellent properties such as high specific strength, good corrosion resistance and excellent biocompatibility^[7,8]. LSF technique has been widely used to manufacture titanium alloy components, in which the LSF Ti-Al-V system alloys are the most widely studied. Carroll et al^[9] investigated the anisotropic mechanical properties of a Ti-6Al-4V three dimensional cruciform component fabricated using a directed energy deposition additive manufacturing (AM) process, and demonstrated that quasi-static uniaxial tensile mechanical properties were similar to those of wrought Ti-6Al-4V. Qiu et al^[10] prepared Ti-6Al-4V samples by direct laser deposition

Received date: February 22, 2018

Foundation item: National Key Basic Research Development Program of China (2016YFB1100103); China Postdoctoral Science Foundation (2016M592731); Fundamental Research Funds for the Central Universities (300102319208, 300102318205); National Training Program of Innovation and Entrepreneurship for Undergraduates (201810710119)

Corresponding author: Yang Haiou, Ph. D., State Key Laboratory of Solidification Processing, Northwestern Polytechnical University, Xi'an 710072, P. R. China, Tel: 0086-29-88494001, E-mail: yanghaiou@nwpu.edu.cn

Copyright © 2019, Northwest Institute for Nonferrous Metal Research. Published by Science Press. All rights reserved.

(DLD) under various processing conditions, and it was found that the as-fabricated microstructure was characterized by columnar grains together with martensite needle-like structure and a small fraction of β phase, which led generally to high tensile strength but low elongation. Banerjee et al.^[11] conducted the precipitation of grain boundary α in a laser deposited and compositionally graded Ti-8Al-xV alloy for an orientation microscopy study. Yan et al.^[12] studied the direct laser deposition of Ti-6Al-4V from elemental powder blends to understand the effects of laser transverse speed and laser power on the microstructure and Vickers hardness of initial deposits.

Mo and V are all the most commonly used β phase stable elements in titanium alloy and Mo is of low cost and low toxicity, and these characteristics prompted us to conduct a preliminary study on Ti-6Al-yMo prepared by LSF, and to explore the application of such alloys^[13]. In fact, recent studies indicate that Ti-6Al-6Mo is a kind of potential material for biomedical application, and the preparation and heat treatment of this alloy were studied. Senopati et al.^[14] synthesized the Ti-6Al-6Mo by arc melting, and investigated the phase stability, mechanical properties, and electrochemical behavior of as cast Ti-6Al-6Mo alloy. Rokhmanto et al.^[15] investigated the influence of solution treatment cooling medium on microstructure and elastic modulus of Ti-6Al-6Mo, and found that the lowest elastic modulus of the alloy quenched in water is 104.7 GPa. Sutowo et al.^[16] investigated the thermo-mechanical treatment process of α/β Ti-6Al-6Mo alloy as new alternative materials for biomedical application.

In the present study, we intend to research the heat treatment system of the novel Ti-6Al-6Mo alloy prepared by LSF with pure Ti, Al and Mo as raw materials, focusing on the effect of solution and aging treatment parameters on the microstructure evolution and micro-hardness of the alloy. The influence of the heat treatment on the microhardness was also discussed.

1 Experiment

The deposited materials used in the experiments were commercially pure Ti, Al and Mo powders with particle sizes of 100~150 μm , 150~250 μm , and 75~125 μm , respectively. The purity of the Ti powder is higher than 99.5%, while that of Al powder and Mo powder are higher than 99.7%. Prior to the experiments, the elemental powder particles were mixed in a ratio of 88wt%Ti+6wt%Al+6wt%Mo and mechanically mixed using a ball mill for 20 min, and then dried at 350 K in vacuum for 24 h to reduce the impact of moisture absorption on the formation quality. The substrate was pure titanium plate with a size of 200 mm \times 50 mm \times 12 mm, which was polished using abrasive paper, and its surface was washed with absolute

ethanol and acetone.

The experiments were carried out with a Prime CP4000 fast axial-flow CO₂ laser, a numeric controlled working table, a high precision powder feeder and a coaxial nozzle with four symmetrical powder nozzle tips. The forming process was conducted in an inert atmosphere processing chamber, where the oxygen content of the forming atmosphere was less than 100 $\mu\text{g/g}$. During the forming process, the laser beam was directed onto the substrate surface to form a moving molten pool. The metal powder particles were delivered into the molten pool synchronously via the powder feeder and coaxial nozzle, and experienced the melting and solidification process to form a deposition layer. The experimental process parameters are shown in Table 1.

A block specimen with 140 mm \times 12 mm \times 10 mm in size was prepared, and 10 block samples (10 mm \times 10 mm \times 5 mm) were cut from the deposition specimen using the wire cutting method, which were used for the heat treatment. The solution and aging treatment were carried out in an SCR box-type high temperature furnace. In order to define the representative solution and aging treatment parameters, the α/β phase transition temperature of Ti-6Al-6Mo was calculated using Thermo-calc (by inputting the composition of the Ti-6Al-6Mo alloy and using the TTTI database, and the α/β phase transition temperature can be directly outputted via the Thermo-calc software). The results confirmed that the theoretical phase transition temperature for Ti-6Al-6Mo is 940.97 $^{\circ}\text{C}$. The temperatures of solution treatment were set at 850 and 920 $^{\circ}\text{C}$, and its respective impacts were examined at 1000 $^{\circ}\text{C}$ which is above the phase transition temperature. Moreover, parameters for solution and aging treatments are shown in Table 2. After the deposition and heat treatment, the metallographic specimens were prepared via standard mechanical polishing means. A solution of HF:HNO₃:H₂O, with a ratio of 1:3:20, was used as an etching agent for all specimens. The microstructure was analyzed using an OLYMPUS-PMG3 metallographic microscope and a Hitachi-S4800 SEM, and the microhardness of these alloy samples was determined using the HX-1000 microhardness tester.

2 Results

2.1 Microstructure of as-deposited Ti-6Al-6Mo

Fig.1 shows the microstructure of as as-deposited Ti-6Al-6Mo. As seen in Fig.1a, the as-deposited Ti-6Al-6Mo is dominated by some big columnar grains and some near-equiaxed grains with a width of 200~500 μm . The grains grow alternately in brightness and darkness, and no metallurgical defects such as lack of fusion were detected in the deposited layer, indicating excellent metallurgical quality.

Table 1 Process parameters of LSF Ti-6Al-6Mo alloy

Laser power/W	Scanning speed/mm·s ⁻¹	Spot diameter/mm	Powder feed rate/g·min ⁻¹	Carrier gas flow rate/L·h ⁻¹	Overlap/%	$\Delta Z/\text{mm}$
2300	6	3.0	10	200	40	0.25

Table 2 Heat treatment parameters of LSF Ti-6Al-6Mo alloy

No.	Solution temperature/°C	Solution time/h	Cooling method	Aging temperature /°C	Aging time/h	Cooling method
A1	850	2	Air	540	4	Air
A2	920	2	Air	540	4	Air
A3	1000	2	Air	540	4	Air
B1	920	4	Air	540	4	Air
B2	920	8	Air	540	4	Air
C1	920	2	Water	540	4	Air
C2	920	2	Furnace	540	4	Air
D1	920	2	Air	540	8	Air
D2	920	2	Air	540	16	Air

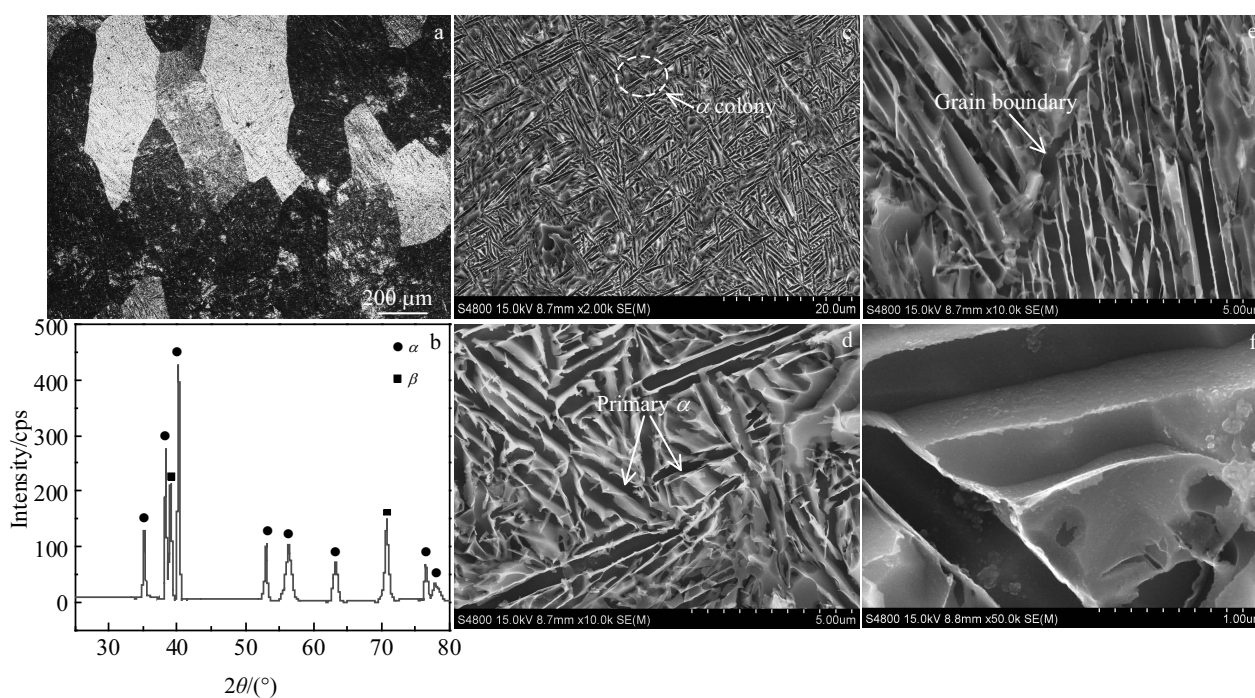


Fig.1 Microstructures of as-deposited Ti-6Al-6Mo fabricated by laser solid forming: (a) morphology of prior β grains, (b) XRD pattern and (c~f) microstructures of prior β grains

Fig.1b shows the typical XRD pattern of as-deposited Ti-6Al-6Mo in the 2θ range of $25^\circ\sim 80^\circ$ to analyze the phase presented in prior β grains. The as-deposited Ti-6Al-6Mo consists of the hexagonal α -Ti phase and cubic β -Ti, without martensite in prior β grains due to the multiple thermal cycles in multi-layer deposition process. Fig.1c and 1d show the microstructure of prior β grains, which is composed of the basketweave α laths with an average width of $\sim 0.5\ \mu\text{m}$ and a length of $2\sim 10\ \mu\text{m}$ and the retained β phase between α laths. Some α laths were arranged parallelly to form a α colony with a width of $1\sim 5\ \mu\text{m}$, which was randomly distributed on the retained β matrix (Fig.1c). It should be pointed out that the grain boundaries of as-deposited Ti-6Al-6Mo are continuous and definite, and these parallel α laths precipitate along the grain boundaries to form α colonies (Fig.1e). As shown in Fig.1f, little precipitation of the secondary α laths was

observed on the retained β matrix under high magnification SEM observation.

2.2 Influence of heat treatment on microstructure

2.2.1 Influence of solution temperature (A1~A3)

Fig.2a~2i show the microstructures of LSF Ti-6Al-6Mo after solution treatment at 850, 920, and 1000°C , followed by air-cooling and aging treatment at 540°C for 4 h, which reveals the influence of solution temperature on the microstructure. It can be seen in Fig. 2a~2c that the morphology and size of the prior β grains are similar to those of as-deposited sample. However, compared with the as-deposited sample, the grain boundaries are somewhat coarsened after the solution aging treatment at 850 and 920°C , and the brightness/darkness alternation between the different grains was weakened, indicating the improved microstructure uniformity between the different grains. When the solution

treatment temperature reaches 1000 °C, the local grain boundaries are significantly coarsened to form a large grain boundary α , as shown in Fig.2c. Fig.2d~2i show the microstructure of prior β grains of the samples after solution and aging treatment (A1~A3 in Table 2). The microstructure of the prior β grains are mainly composed of basketweave primary α laths, the retained β matrix, and very fine secondary α laths precipitated from the β matrix. As seen in Fig.2d, when the solution temperature is 850 °C, the size of the primary α laths changes little compared to that of as-deposited sample, and a small amount of secondary α laths are precipitated on the retained β matrix. When the solution temperature rises to 920 °C (Fig. 2e and 2h), numerous secondary α laths precipitate on the β matrix with an average width of $\sim 0.02 \mu\text{m}$ and a length of $0.1\sim 0.5 \mu\text{m}$, and the size of the primary α laths increases to $\sim 1.2 \mu\text{m}$. It is worth noting that when the solution temperature reaches 1000 °C, both the primary α laths and secondary α laths are coarsened significantly, and a few primary α laths are transformed into globular α with an average diameter of $\sim 10 \mu\text{m}$, as shown in Fig.2f and 2i.

Fig.3 shows that the microhardness HV of the solution and

aging treated sample increases from 4210 MPa to 4340 MPa when the solution temperature rises from 850 °C to 920 °C, and the microhardness reaches the highest value at 920 °C. When the solution temperature rises to 1000 °C the microhardness decreases to 3870 MPa. The results show that the solution temperature has a significant effect on the microhardness of the alloy.

2.2.2 Influence of the solution time (A2, B1, B2)

Fig.4a~4f show the microstructures of LSF Ti-6Al-6Mo after solution treatment at 920 °C for 4 and 8 h, followed by air cooling and aging treatment at 540 °C for 4 h. As seen from the microstructure of the A2, B1 and B2 samples, the morphology of prior β grains changes little with increasing the solution time from 2 h to 8 h, but the local grain boundaries are considerably coarsened, forming a large grain boundary α , as shown in Fig.4a and 4b. Meanwhile, when the solution time increases from 2 h to 8 h, the size of the primary α laths and the amount of secondary α laths increase gradually, and some α laths are coarsened with a tendency to transform into globular α at the solution time of 8 h (as indicated by the arrows in Fig.4c and 4d). From Fig.4e and 4f, it can be found that the

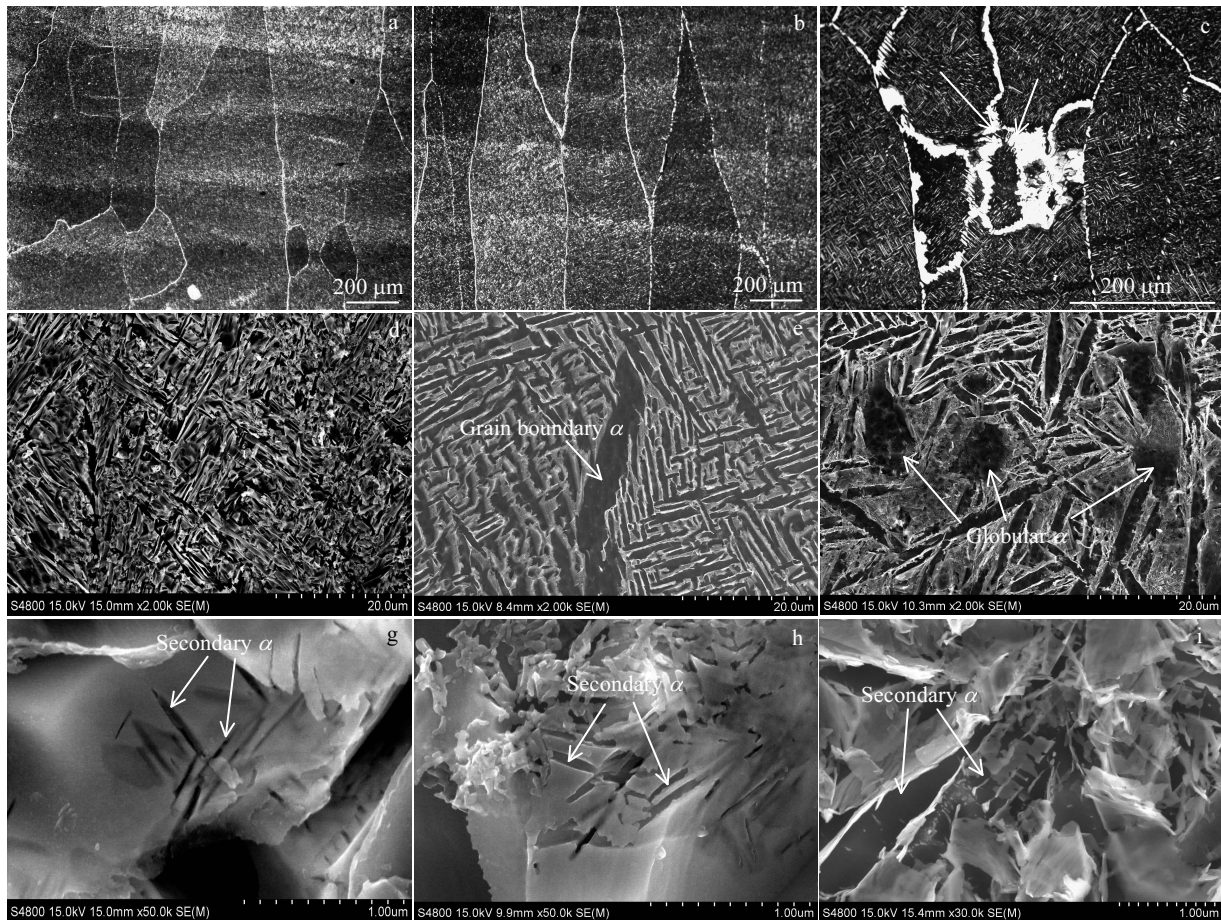


Fig.2 Microstructures of LSF Ti-6Al-6Mo after solution treatment at different temperatures, followed by air-cooling and aging treatment: (a, d, g) 850 °C, (b, e, h) 920 °C, and (c, f, i) 1000 °C

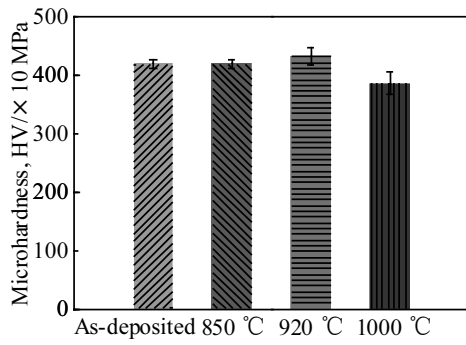


Fig.3 Microhardness of as-deposited and solution treated samples at different temperatures

amount of the secondary α laths in the sample solution treated

for 4 and 8 h increases obviously compared to in the sample solution treated for 2 h.

From Fig.5, it can be seen that when the solution time increases from 2 h to 8 h, the microhardness HV of the alloy firstly reaches a maximum value of 4670 MPa at 4 h and then decreases very slightly to 4640 MPa at 8 h. The results show that the solution time has no significant effect on the microhardness of the alloy when the solution time exceeds 4 h.

2.2.3 Influence of the cooling method (C1, A2, C3)

After the solution treatment, the cooling method may markedly impact the formation of the alloy microstructure. Based on this conjecture, the impact of three different cooling methods (water cooling, air cooling, and furnace cooling) on the alloy microstructure was systematically studied after the solution treatment at 920 °C for 2 h. Fig.6a~6f show the microstructures after air cooling, water cooling, and furnace

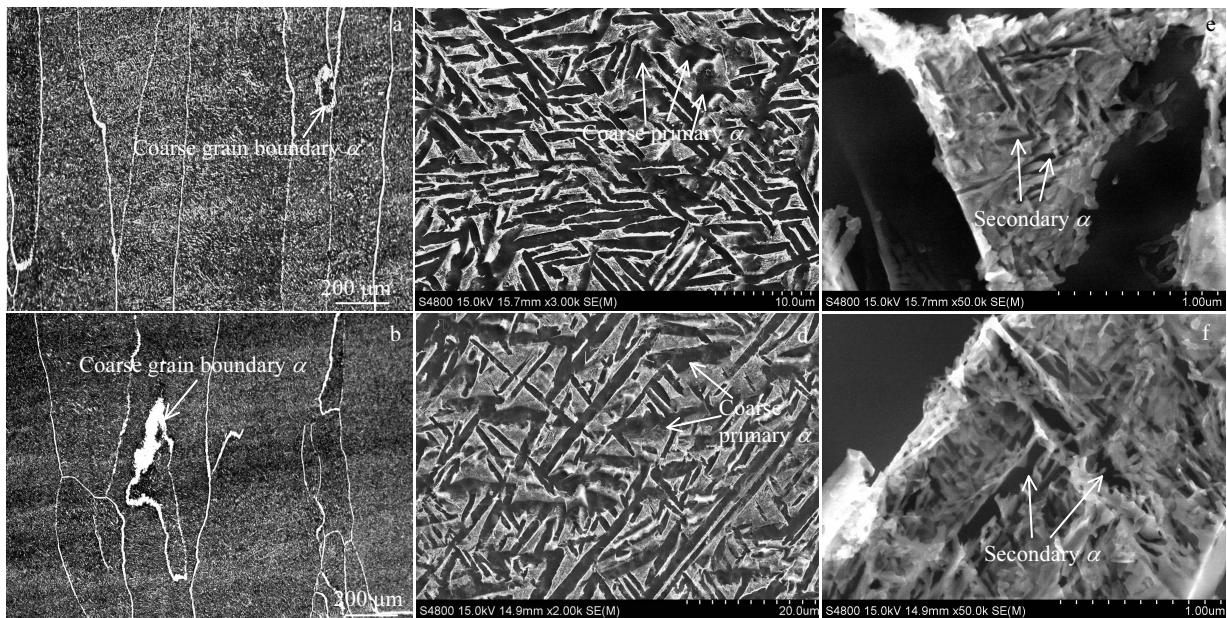


Fig.4 Microstructure of LSF Ti-6Al-6Mo after solution treatment at 920 °C for different time, followed by air cooling and aging treatment: (a, c, e) 4 h and (b, d, f) 8 h

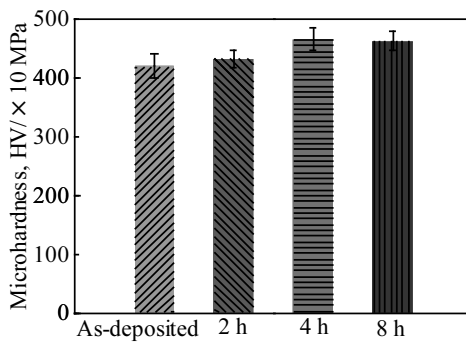


Fig.5 Microhardness of as-deposited and solution treated samples at 920 °C for different time

cooling after the solution treatment at 920 °C for 2 h, followed by air cooling and aging treatment at 540 °C for 4 h. Local large grain boundary α is also found in the sample after the solution + furnace cooling and aging treatment. The average width of primary α laths after solution+water cooling is $\sim 0.8 \mu\text{m}$, which is much smaller than that of the air cooled samples. A highly dispersed secondary α laths are precipitated on the β matrix with an average width of $0.08 \mu\text{m}$. In addition, the microstructure of the sample treated by solution+furnace cooling is very different from that treated by solution+air cooling and solution+water cooling. The large-sized primary α laths with an average width of $\sim 1.5 \mu\text{m}$ are distributed on the retained β matrix while no obvious secondary α laths are detected.

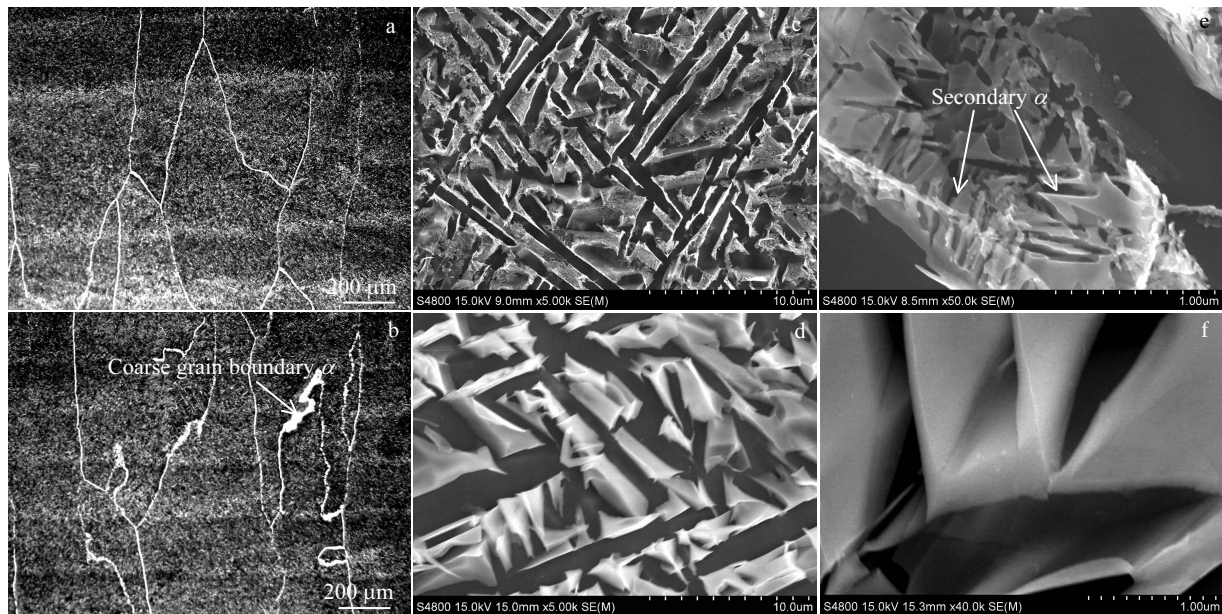


Fig.6 Microstructures of LSF Ti-6Al-6Mo after solution treatment at 920 °C for 2 h, followed by different cooling methods and aging treatment: (a, c, e) water cooling and (b, d, f) furnace cooling

It can be seen from Fig.7 that the microhardness of the sample after water cooling is the highest, and that of the sample after the furnace cooling is the lowest, indicating that the cooling method has a great influence on the microhardness of the alloy.

2.2.4 Influence of the aging time (A2, D1, D2)

Fig.8a~8f show the typical microstructures of the Ti-6Al-6Mo sample prepared by LSF after solution treatment at 920 °C for 2 h, followed by aging treatment at 540 °C for different time (4, 8 and 16 h). After being aged for 2 h, the grain boundary α is significantly coarsened, while the microstructure of prior β grains is still composed of the retained β matrix, the primary α laths with an average width of $\sim 1 \mu\text{m}$, and the secondary α laths with an average width of $\sim 0.02 \mu\text{m}$. This indicates that the aging time has a relatively small

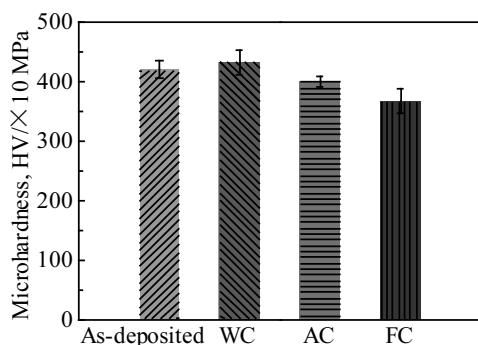


Fig.7 Microhardness of as-deposited sample and solution treated sample at 920 °C for 2 h followed by different cooling methods (AC: air cooling, WC: water cooling, FC: Furnace cooling)

influence on grain boundaries and the microstructure of Ti-6Al-6Mo when the aging time exceeds 4 h.

As can be seen from Fig.9, the microhardness HV of Ti-6Al-6Mo reaches a maximum value of 4340 MPa at 4 h of aging time and remains almost constant with an increase in aging time. The results show that prolonging the aging time has little effect on the microhardness of the alloy.

3 Discussion

The microhardness of the alloy is closely related to the morphology, size, and distribution of the primary α phase and the secondary α phase. In particular, the secondary α laths significantly hinder the dislocation movement and increase the hardness and strength of the sample due to their small size and randomly distributed orientations. As shown in the microstructure of as-deposited sample and heat treated samples in this study, a large amount of secondary α laths are precipitated in retained β matrix except the as-deposited sample and the sample that undergoes solution and furnace cooling followed by aging. Firstly, the mechanism of the microstructure formation will be discussed combining the heat treatment process. Fig.10 presents the schematic of the microstructure formation during a typical heat treatment process in this study. It can be seen that as a result of rapid cooling during the LSF process, supersaturated basketweave α laths are formed in as-deposited sample and large residual stress and deformation energy are generated in the sample. During the solution and aging treatment, when the sample is heated to a temperature close to the phase transition temperature, some primary α laths are dissolved and the number of the primary α laths is reduced due to higher diffusion

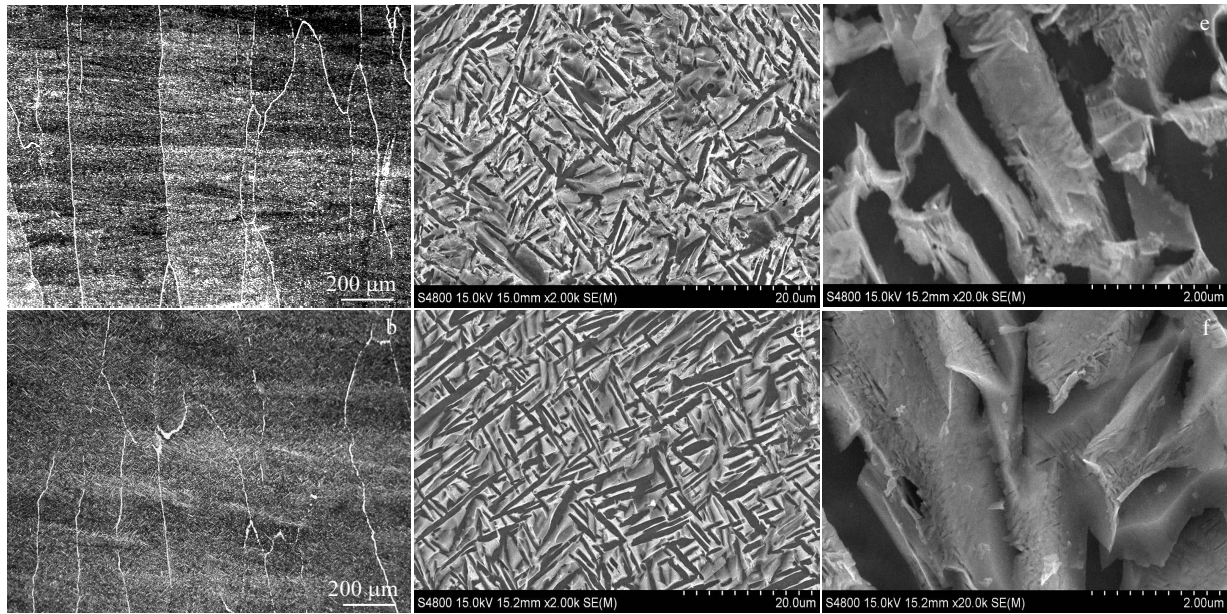


Fig.8 Microstructures of LSF Ti-6Al-6Mo after solution treatment at 920°C for 2 h, followed by aging treatment at 540°C for different time: (a, c, e) 8 h and (b, d, f) 16 h

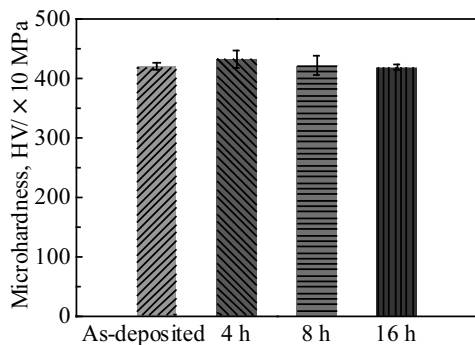


Fig.9 Microhardness of as-deposited and heat treated samples at 920 °C for 2 h followed by aging treatment at 540 °C for different time

coefficients and increased atomic activity. When the temperature of the solution is very close to or slightly higher than the temperature of the phase transition temperature, some primary α laths begin to become spheroids because of the release of residual stress at high temperatures.

In the subsequent cooling process, when furnace cooling is conducted after solution treatment at 920°C, the primary α is coarsened due to the slow cooling rate, forming the relatively large basketwave primary α laths or primary α laths and some spherical α distributed on the β matrix. When the water cooling or air cooling is carried out after solution treatment, the cooling rate is quite high (air cooling can also achieve a very high cooling rate because of the very small sample size used in this study), and the Mo content in retained β phase is

close to its critical concentration in titanium, so a large amount of dispersed ω phase will be precipitated on the retained β matrix after the water or air cooling process. In the next step, during the aging treatment, the dispersed ω phase will transform into the very small secondary α laths and retained β , and thus the microstructure, which is composed of primary α laths, a large quantity of very small secondary α laths and the retained β , is obtained after the solution followed by air or water cooling and aging treatment.

In order to correlate the microhardness with the microstructure of the samples after heat treatment, the strengthening effect of the primary α laths and secondary α laths will be further discussed, as shown in Fig.11. During the deformation process, due to the enrichment of dislocations in the α/β phase boundary, the dislocation density increases as the size of the α laths decreases and the orientation of the α laths increases. So the strength and hardness of the alloy increase with the decrease in the size of α laths due to the increase in local dislocation tangles and dislocation densities, as shown in Fig.11a and 11b. When the size and number of primary α are constant, and the secondary α precipitates on the retained β matrix, the dislocation density can be significantly increased due to the very small size of the secondary α and the random distribution of the orientation, which leads to local dislocation intersection and dislocation multiplication. Therefore, secondary α will definitely increase the strength and hardness of the alloy as a strengthening phase. Moreover, it can be concluded that the strengthening effect of the secondary α laths is stronger than that of the primary α laths.

By combining Fig.10 and Fig.11, the effects of the solution

time, solution temperature, cooling method and aging time on the microhardness of the alloy can be easily explained. As the solution temperature increases from 850 °C to 920 °C, the microhardness reaches the highest. This can be explained by the fact that the secondary α laths precipitated on the retained β matrix at 920 °C are more than at 850 °C, and when the temperature reaches 1000 °C, both the primary α laths and the secondary α laths are coarsened and lead to the decrease of the microhardness. Since the amount of secondary α laths increases firstly and then keeps almost constant as the solution time increases from 2 h to 8 h, the microhardness increases first and then keeps constant with increasing the solution time. When the alloy is water cooled, the smaller primary α laths are obtained and a highly dispersed secondary α laths are precipitated on the retained β phase compared to air cooling, and the highest microhardness of the alloy is achieved. Since no obvious secondary α phase is detected on the retained β matrix after furnace cooling treatment, the microhardness of the sample after furnace cooling is the lowest. When aging time exceeds 4 h, the microstructure becomes more homogeneous. Therefore, the microhardness keeps almost constant when the aging time exceeds 4 h.

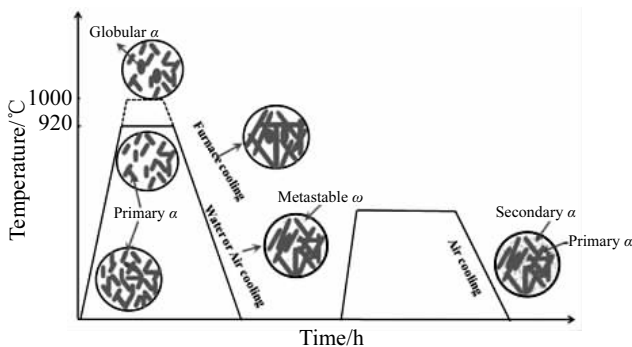


Fig.10 Schematic of the precipitation of primary α and secondary α phases of LSF Ti-6Al-6Mo alloy sample after solution and aging treatment

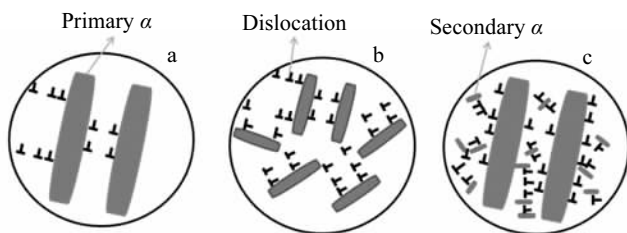


Fig.11 Schematic of the influence mechanism of primary α and secondary α laths on the dislocation movement

4 Conclusions

1) When LSF Ti-6Al-6Mo samples is solution treated at temperatures of 850~1000 °C for 2~8 h followed by air cooling or water cooling and aging treatment, the microstructure of prior β grains is composed of primary α laths, secondary α laths and retained β matrix. The size of primary α laths and secondary α laths increases with solution temperature. It also increases with the solution time at first, and then keeps almost constant. The finest primary α laths and secondary α laths are obtained after solution treatment at 920 °C for 2 h, followed by water cooling and aging treatment, while no secondary α lath is found after solution treatment followed by furnace cooling.

2) The microhardness of LSF Ti-6Al-6Mo decreases with the increase of the size of primary α laths. It also increases as the amount of secondary α laths increases and the size of secondary α decreases. The strengthening effect of the secondary α laths is stronger than that of primary α laths.

References

- Emamian A, Farshidianfar M H, Khajepour A. *Journal of Alloys and Compounds*[J], 2017, 710(5): 20
- Cao S N, Gu D D, Shi Q M. *Journal of Alloys and Compounds*[J], 2017, 692: 758
- Zhong C L, Chen J, Linnenbrink S et al. *Materials & Design*[J], 2016, 107: 386
- Mahamood R M, Akinlabi E T. *The International Journal of Advanced Manufacturing Technology*[J], 2017, 91(5-8): 2419
- Gasper A N D, Catchpole-Smith S, Clare A T. *Journal of Materials Processing Technology*[J], 2017, 239: 230
- Zhang F Y, Yang M, Clare A T et al. *Journal of Alloys and Compounds*[J], 2017, 727: 821
- Cai C, Song B, Xue P J et al. *Journal of Alloys and Compounds*[J], 2016, 686: 55
- Cai C, Gao Y X, Teng Q et al. *Materials Science and Engineering A*[J], 2018, 217: 95
- Carroll B E, Palmer T A, Beese A M. *Acta Materialia*[J], 2015, 87: 309
- Qiu C L, Ravi G A, Dance C et al. *Journal of Alloys and Compounds*[J], 2015, 629: 351
- Banerjee R, Bhattacharyya D, Collins P C et al. *Acta Materialia*[J], 2004, 52(2): 377
- Yan L, Chen X Y, Li W et al. *Rapid Prototyping Journal*[J], 2015, 22(5): 810
- Zhang F Y, Chen H, Xu Y K et al. *Rare Metal Materials and Engineering*[J], 2013, 42(7): 1332
- Senopati G, Putrayasa I N G, Sutowo A C. *IOP Conference Series: Materials Science and Engineering*[J], 2017, 202: 012034
- Rokhmanto F, Muzakif A, Alhamidi A A. *AIP Conference Proceedings*[J], 2018, 1964: 020049
- Sutowo C, Rokhmanto F, Senopati G. *Widyariset*[J], 2017, 3(1): 47

热处理对激光立体成形新型 Ti-6Al-6Mo 合金显微组织和硬度的影响

张凤英¹, 胡腾腾¹, 谭 华², 邱 莹¹, 梅 敏¹, 杨海欧²

(1. 长安大学, 陕西 西安 710064)

(2. 西北工业大学 凝固技术国家重点实验室, 陕西 西安 710072)

摘 要: 以混合元素粉末为原料, 采用激光立体成形 (Laser solid forming, LSF) 技术制备新型 Ti-6Al-6Mo 合金。研究了沉积态试样的显微组织以及固溶时效处理对合金显微组织形成及硬度的影响。结果表明, 本研究所采用的热处理制度对原始 β 晶粒形貌没有显著的影响; 固溶温度、固溶时间和固溶后的冷却方式对原始 β 晶粒中 α 相的形貌和尺寸以及 LSF Ti-6Al-6Mo 合金的显微硬度均有显著影响。当时效时间超过 4 h 后, 随着时效时间的延长, 合金的显微组织和显微硬度均未产生明显变化。基于不同热处理条件下 LSF Ti-6Al-6Mo 合金中初生 α 板条和次生 α 板条的析出机制及其对 β 基体的强化作用分析, 揭示了热处理对 LSF Ti-6Al-6Mo 合金的显微组织和显微硬度的影响机理。

关键词: 激光增材制造; Ti-6Al-6Mo; 热处理; 微观组织; 显微硬度

作者简介: 张凤英, 女, 1980 年生, 博士, 教授, 长安大学材料科学与工程学院, 陕西 西安 710064, 电话: 029-82337340, E-mail: zhangfengying@chd.edu.cn